ARMA 11-0175

Design Concept for Perimeter Control Blasting in Drifting Operations

Iverson, S. R. and Hustrulid, W. A.
OMSHR NIOSH, Spokane, Washington, USA

This paper was prepared for presentation at the San Francisco, 2011, 45th US Rock Mechanics / Geomechanics Symposium, held in San Francisco, CA, June 26–29th, 2011.

ABSTRACT: NIOSH has recently concluded an extensive blasting research and development program. One objective was to develop practical tools that encourage and facilitate the use of perimeter control in drift driving. NIOSH research suggests that proper design of the buffer row of the blastholes is the key to successful perimeter control. Specifically, if the buffer row of holes has been properly designed, the perimeter row of holes simply will do the final smoothing and shaping. Three blast damage models are presented and two blast design examples are described using model predictions. The paper concludes with recommendations for collecting the field experience to determine the optimum practical damage radius.

The findings and conclusions in this paper are those of the authors and do not necessarily represent the official position of the National Institute for Occupational Safety and Health.

1. INTRODUCTION

Drift driving has always been an important part of underground mining. With the development of powerful drill jumbos, the introduction of bulk explosives in the 1980s, and the introduction of many new types of rock reinforcement, the overall process of rock excavation and support became very productive. An unintended consequence of advancements in extraction capability has often been less control of the extent of the damage to the surrounding rock, creating less stable ground control environments at times.

Today, some mines are placing more focus on the need to control the geometry of the drift opening using controlled blasting. Methods include the use of decoupled charges for back holes, short bottom charges to reduce the overall hole pressure, and the use of line drilling empty holes at the perimeter to provide a free face to stop perimeter damage. These methods are a positive development for both economic and safety considerations. To help achieve improvements in perimeter control, better strategies must be made available to the mining industry.

The National Institute of Occupational Safety and Health (NIOSH), as part of an effort to reduce accidents and injuries caused by falls of ground, has recently concluded an extensive research and development program aimed at improving blasting practices during drift driving. Poor blasting practices, which result in excessive overbreak and rock damage, are a possible contributing factor in these accidents. One specific objective has been to develop practical tools that encourage and facilitate the use of perimeter control in drift driving. The authors suggest that the proper design of the buffer row of blastholes is the key to successful perimeter control. If the buffer row of holes is properly designed, the perimeter row of holes simply must do the final smoothing and shaping. A number of different blast design approaches were investigated with the intent to provide an easy-to-use drift blast design software package that will allow engineers to study the complex interactions of blast design factors such as hole diameter, explosive properties, and careful perimeter blasting strategies, with the overall goal of reducing unnecessary overbreak and wall rock damage.

A software tool was developed which contains algorithms and blast damage models to be used in design [1]. In the case of controlled blasting, the algorithm includes a selection of explosives and a location of holes that minimizes damage to the perimeter yet provides for extraction of the rock up to the perimeter. The software is available from the authors as a beta version. There are no plans to complete the software product.

This paper describes the buffer algorithm for the software and provides a detailed look at the equations for three practical blast damage approaches. A successful controlled blast design was analyzed using these damage models. Two successful blasts are analyzed and recommendations are provided for collecting the field experience needed to implement a buffer design.

2. BUFFER ROW ALGORITHM

2.1. *Traditional controlled blast design*

Perimeter control blasting is commonly applied to the roof but increasingly it is being applied to the walls as well. Figure 1 illustrates, based on literature, the different design sectors commonly distinguished for a drift round.

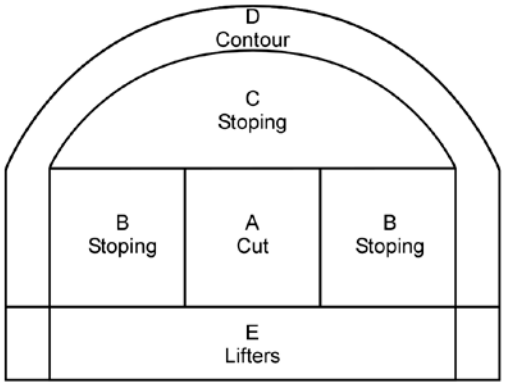

Figure 1. Diagrammatic representation of the design sectors involved in a drift round. After Holmberg [2].

As can be seen, a significant burden is assigned to the contour row in the Figure 1 design. To better understand the traditional approach to perimeter control, the following is a description of the algorithm. One begins by designing the cut, the contour, and the lifter sectors. When the particular designs for each of the sectors have been completed, they are added to the overall drift design. The so-called stoping holes are then added as needed. The implication is that the holes/explosives included in the different sectors are responsible for removing the associated rock. In the case shown in Figure 2, the width (the "burden") of the contour sector is denoted as B. Particularly in a hard, strong rock, it is expected that the amount of explosive charge required to remove the contour sector of rock is high, and subsequently would place strong requirements on the perimeter row design. For the Holmberg design shown in Figure 1, the perimeter burden is simply determined based on the spacing of the perimeter holes. Holmberg suggests analysis of the stoping, buffer, and perimeter holes for perimeter damage using critical peak particle velocity. The damage extent is illustrated in Figure 3.

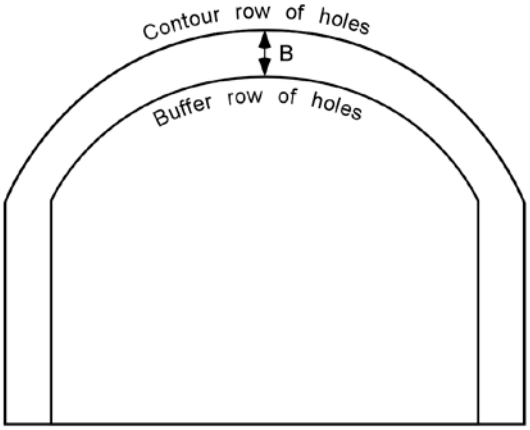

Figure 2. Contour sector bounded by the contour row and the buffer row.

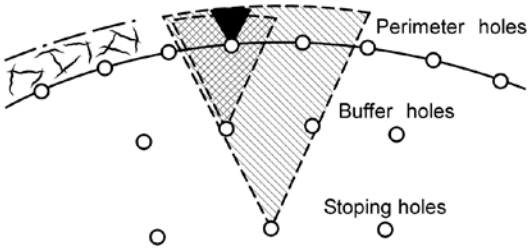

Figure 3. The charge concentrations in the holes close to the contour are adjusted so that the damage zone from each hole coincides. After Holmberg [2].

2.2. *Buffer hole concept*

The buffer hole concept is different than that used in traditional perimeter control blast design. The contour sector is not determined by the perimeter charges but is instead determined by charges along the inside edge of the contour sector (Figure 2). The buffer concept was first published by Hustrulid and Johnson [3]. The contour strip of rock is bounded on the inside by the buffer row of holes and on the outside by the perimeter (contour) row of holes. The detonation of the buffer row will produce damage in the contour sector. As will be discussed in some detail later, the idea is to design the buffer holes so that their associated damage radius (R_d) extends to the desired drift perimeter. Figure 4 shows the case when:

R_d = contour row "burden."

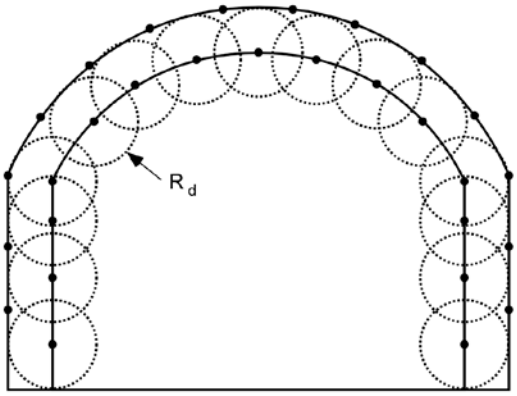

Figure 4. The damage radius for the buffer holes are shown to just touch the perimeter.

In this case, after the firing of the buffer holes, the amount of fresh/undamaged rock is only the small cusp of rock remaining between damage circles. The authors suggest a buffer hole spacing of $1.3R_d$ to $1.5R_d$ to minimize cusp size. Thus, the breaking demand on the perimeter holes is substantially reduced and a prime reason why the use of high-strength detonating cord often functions well as a perimeter control explosive since the primary function has become one of smoothing rather than primary breaking. The first buffer holes are placed at the abutment corners and the remaining buffer holes spaced according to the above spacing suggestion. Perimeter holes are placed beginning with the abutment corners and spaced according to the buffer hole cusp locations. The spacing design is well-illustrated in Figure 4.

The design of the perimeter, buffer, and stoping holes in breaking the contour sector of rock as proposed by the Holmberg approach, as shown in Figure 3, results in eventually damaging the perimeter rock. The buffer design only uses the buffer and perimeter holes to remove the contour sector of rock and minimizes damage to the perimeter.

Interestingly, the stoping holes pre-condition the contour sector and is supported by Tesarik et al. [4], who found through analysis of peak particle velocities that blast damage occurs beyond the subsequent row to be detonated. At this point in time, the proposed buffer hole concept does not necessarily consider damage caused from a previous delay in determining the next row's blast damage radius. It could be argued that empirical-based damage models do account for the described preconditioning.

2.3. *The damage radius*

The key to the buffer algorithm described by Hustrulid and Johnson [3] is the application of a "practical damage radius" (R_d) to each blasthole/explosive combination. By "practical," it is meant that if the rock mass lying outside of the ring were removed, the rock remaining within the ring would easily break apart. As can be seen in Figure 5, the practical damage zone consists of both crushing and cracking components.

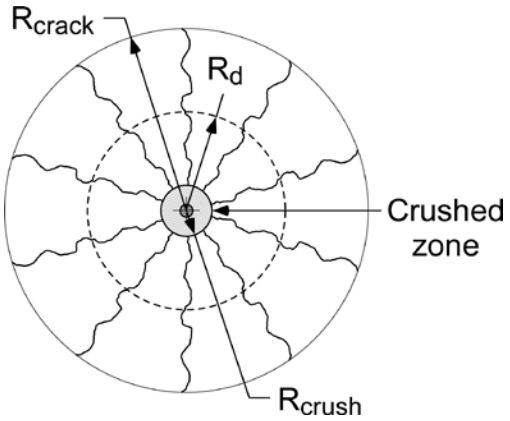

Figure 5. Diagrammatic representation of the crushed zone, the cracked zone, and the practical damage radius surrounding a blast hole.

2.4. *Explosives availability and properties*

Perimeter charging options for the buffer design require careful consideration, since such a choice may be a dramatic change for a mine. A decoupled perimeter charge is necessary to implement the buffer algorithm. Without perimeter control, damage typical of an aggressive blast will result. Explosives manufacturers have products suited for perimeter control; two examples are detonation cord, which comes in various charge concentrations, and emulsion-based trim cartridges or continuous charges. An alternative option is to use the current explosive (pumped emulsion or blown ANFO) as a bottom charge. Limiting the explosive to a bottom charge reduces the overall energy in the perimeter hole. The use of detonators, boosters, or cartridges for initiation of the column charge is not considered in the algorithm.

2.5. *Drift geometry*

The geometry of the drift does not change when using the buffer algorithm. The buffer algorithm is adapted to the desired perimeter outcome and can be applied to any drift design. The diameter of the blast hole is a necessary input for determining blast damage for all of the damage models. The length of the blast holes and the resulting length of the blast round are not considered in the buffer algorithm. The design considers the buffer and perimeter holes to be drilled parallel.

2.6. *Rock properties*

The rock type to be blasted will directly affect the outcome and is considered in various levels of complexity in the blast damage models. If the engineer can only provide rock density, then that is sufficient to run two of the three damage models described later.

3. DETAILED DESCRIPTIONS OF SELECTED BLAST DAMAGE MODELS

Several blast damage models described in the literature have been reviewed for possible use in determining the practical damage limit for the buffer row concept. Three models have been selected for application: Modified Ash energy-based, modified Ash pressure-based, and the Sher mechanics-based. Of these, the Ash-based models are the simplest to apply and are empirically based. The Sher model is based on the principles of solid mechanics and therefore more fundamentally based.

The Ash models utilize empirical results from surface operations. The choice of pressure or energy is available. The Sher model has a quasi-static mechanics basis and requires a comprehensive list of rock properties. In situ stress has been included to make the mechanics derivation complete but has not been utilized. The Sher model provides similar results to the Ash models.

3.1. *Modified Ash Energy-Based Approach*

The modified Ash energy-based approach for calculation of the R_d damage limit can be used as an approximation for damage. In 1963, Ash [5, 6, 7, 8] published his now classic papers dealing with blast design in open pit mines and quarries. Figure 6 is an isometric representation of a bench with the design parameters indicated.

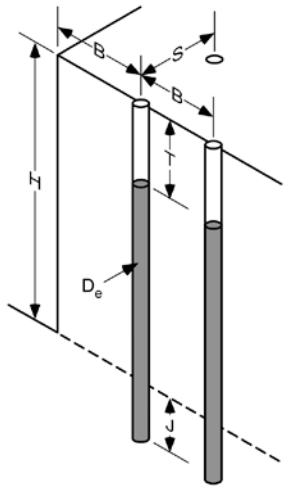

Figure 6. Isometric view of a bench blast design

Using field data collected from a large number of operations, Ash summarized the different design parameters. He found that the sub-drill (*J*), the stemming (*T*), the spacing (S), and the bench height (*H*) could all be related to the burden (*B*). Most importantly, he found that for fully charged holes the burden (*B*) was related to the blasthole diameter (D_e):

$$B = K_B D_e \qquad (3.1)$$

where

B = burden

K_B = constant

D_e = hole diameter

The value of K_B varied with both the rock and the explosive. Ash provided the following recommendations:

- For light explosives in dense rock use $K_B = 20$
- For heavy explosives in light rock use $K_B = 40$
- For light explosives in average rock use $K_B = 25$
- For heavy explosives in average rock use $K_B = 20$

Over time, his work has been shown to have successfully quantified the burden requirements for blasting and today, if one examines open pit/quarrying experience, one finds that with the possible exception of the hole spacing relationship, the ratios are largely followed. In 1999, Hustrulid [9, 10] as part of his book *Blasting Principles for Open Pit Mining*, proposed a design procedure based on energy coverage. It was assumed that the holes were completely charged with explosive, i.e. fully coupled. The radius of the damage circle was obtained by equating available explosive energy to that required to produce acceptable fragmentation. In this regard, it was assumed that the use of ANFO with density 0.85 g/cm^3 to blast an average rock of density 2.65 g/cm^3 yielded satisfactory results when $K_B = 25$. The formula expressing the ratio K_B for other rock-explosive combinations becomes:

$$K_B = 25\sqrt{\frac{\rho_e \; s_{ANFO}}{\rho_{ANFO} s_{1ANFO}}}\sqrt{\frac{2.65}{\rho_{rock}}} \qquad (3.2)$$

where

ρ_e = density of the explosive used (g/cm^3)

s_{ANFO} = weight strength of the explosive relative to ANFO

ρ_{ANFO} = density of ANFO = 0.85 g/cm^3

s_{1ANFO} = weight strength of ANFO relative to ANFO = 1

ρ_{rock} = density of the rock mass (g/cm^3)

Equation (3.2) provides values of K_B that are roughly in keeping with the Ash recommendations regarding the effect of explosive energy and rock density. Based simply on the geometry of just-touching circles

$$B = 2R_d \qquad (3.3)$$

the basic Ash burden formula becomes

$$B = 2R_d = K_B \cdot D_e = K_B \cdot 2\, r_h$$

where

r_h = hole radius

or

$$R_d = K_B\, r_h \tag{3.4}$$

Finally, one obtains the relationship

$$\frac{R_d}{r_h} = 25\sqrt{\frac{\rho_e\ s_{ANFO}}{\rho_{ANFO}}}\sqrt{\frac{2.65}{\rho_{rock}}} \tag{3.5}$$

It is recognized that

$$\frac{\rho_e\ s_{ANFO}}{\rho_{ANFO}} = RBS \tag{3.6}$$

where

RBS = bulk strength relative to ANFO

The *RBS* value is often provided by explosive suppliers. Thus equation (4.5) becomes

$$\frac{R_d}{r_h} = 25\sqrt{RBS}\sqrt{\frac{2.65}{\rho_{rock}}} \tag{3.7}$$

Figure 7 is a simple design curve that can be used to solve for R_d/r_h given the *RBS*. It assumes fully coupled charges and a rock density of 2.65 g/cm^3.

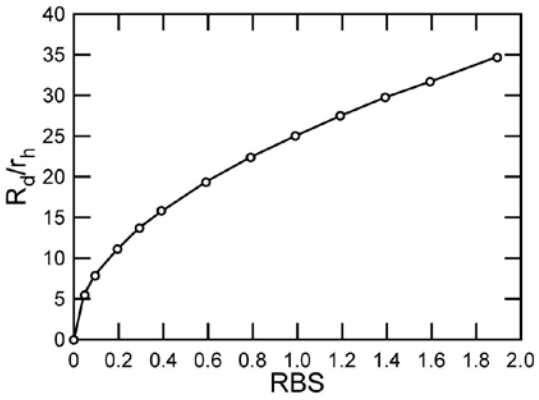

Figure 7. Plot of R_d/r_h versus RBS for the Modified Ash energy-based approach

As can be seen, the approach is quite simple involving available explosive properties and the density of the rock as inputs. Thus, the formula is attractive for mine application. Since it is based on the Ash burden formula and energy factors, it has been given the name "Modified Ash energy-based approach."

Equation (3.5) can be adapted for use with de-coupled charges. The general equation is:

$$\frac{R_d}{r_h} = 25\sqrt{\frac{\rho_e\ s_{ANFO}}{\rho_{ANFO}}\left(\frac{A_e}{A_h}\right)}\sqrt{\frac{2.65}{\rho_{rock}}} \tag{3.8}$$

where

A_e = cross-sectional area of the explosive

A_h = cross-sectional area of the hole

If the explosive is in a cylindrical package and extends the length of the hole, equation (3.8) can be written as:

$$\frac{R_d}{r_h} = 25\left(\frac{d_e}{d_h}\right)\sqrt{\frac{\rho_e\ s_{ANFO}}{\rho_{ANFO}}}\sqrt{\frac{2.65}{\rho_{rock}}} \tag{3.9}$$

3.2. *Modified Ash Pressure-based Approach*

In the previous section, it was assumed that the Ash recommendations could be extrapolated to other explosives and rock types based on energy. One can argue that some other parameter should be used instead. One logical parameter is the borehole wall pressure. Here, the foundation for developing such a relationship is the thick-walled cylinder approximation for a pressurized borehole. It can be shown that:

$$\frac{R_d}{r_h} = 25\sqrt{\frac{P_{e\ wall}}{1300}} \tag{3.10}$$

where

$P_{e\ wall}$ = the borehole wall pressure for the explosive (MPa)

1300 MPa = borehole wall pressure for a fully-coupled charge of ANFO (ρ_{ANFO} = 0.85 g/cm^3 and *VOD* = 3500 m/s)

The explosive wall pressure is general and applies both for fully coupled and de-coupled charges. For the case of de-coupled charges, the co-volume approach is used to calculate the wall pressure [11]. It is noted that equation (3.10) does not include any dependence on the rock mass. To address the lack of rock dependance, the same rock density obtained in developing the energy approach has been included. The final equation becomes:

$$\frac{R_d}{r_h} = 25\sqrt{\frac{P_{e\ wall}}{1300}}\sqrt{\frac{2.65}{\rho_{rock}}} \tag{3.11}$$

Equation (3.11) seems to better reflect the effect of explosive "heaviness (bulk strength)" on the R_d/r_h factor as described by Ash by comparison to the energy approach. However, it is clear that other approaches should be considered. Figure 8 is a simple design curve relating R_d/r_h to the wall pressure for rock of density:

$$\rho_{rock} = 2.65\ \text{g/cm}^3.$$

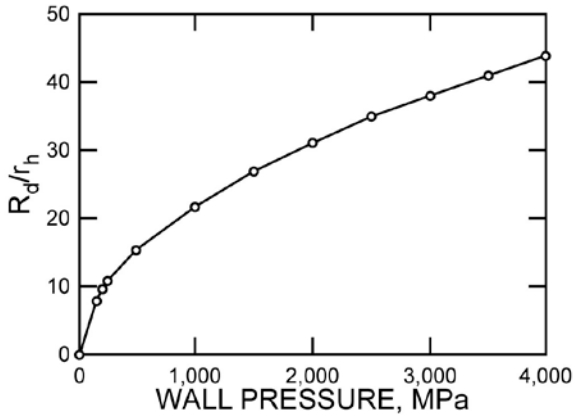

Figure 8. Plot of R_d/r_h versus wall pressure for the Modified Ash energy-based approach.

3.3. *The Sher Quasi-Static Approach*

Sher and co-workers [12, 13, 14] have written several papers concerning the development of the damage zones surround a cylindrical charge. It is a pressure based approach and assumes that the charge is fully coupled. For derivation details, the interested reader is referred to the papers included in the reference list or the author. The relevant equations are presented and their application demonstrated.

The basic equations are:

$$\left(\frac{Y}{\alpha}-q\right)\left(\frac{b}{a}\right)^{\alpha/(1+\alpha)}-\frac{Y}{\alpha}-p(a)=0 \qquad (3.12)$$

$$q=-\frac{Y_2+2P(1+\alpha_2)}{2+\alpha_2} \qquad (3.13)$$

$$u_b=-\frac{(1+\nu)\,b\,[q+2P(1-\nu)]}{E} \qquad (3.14)$$

$$a^2-a_o^{\,2}=b^2-(b-u_b)^2 \qquad (3.15)$$

where

$$\alpha=\frac{2\sin\phi}{1-\sin\phi}$$

$$Y=\frac{2c\cos\phi}{1-\sin\phi}$$

$$\alpha_2=\frac{\sigma_c}{\sigma_t}-1$$

$$Y_2=\sigma_c$$

c = cohesion (MPa)

φ = angle of internal friction (degrees)

E = Young's modulus (MPa)

υ = Poisson's ratio

σ_c = compressive strength (MPa)

σ_t = tensile strength (MPa)

$p(a)$ = borehole wall pressure (MPa) as a function of the radius a

P = in situ stress directed radially inward (MPa)

a_o = initial radius of hole = charge radius (m)

a = final hole radius (m)

b = final outer radius of the crushed zone (m)

u_b = elastic deformation of the surrounding rock mass due to the internal pressurization and the external pressure (in situ stress), m

The gas pressure in the cavity is determined based on the Jones-Miller adiabatic curve given below:

$$p(a)=P_o\left(\frac{a}{a_o}\right)^{-2\gamma_1}, \quad a\le a^* \qquad (3.16a)$$

$$p(a)=P_o\left(\frac{a^*}{a_o}\right)^{-2\gamma_1}\left(\frac{a}{a^*}\right)^{-2\gamma_2}, \quad a\ge a^* \qquad (3.16b)$$

where

P_o = initial wall pressure due to the explosion

γ_1 = initial adiabatic expansion constant = 3

γ_2 = final adiabatic expansion constant = 1.27

a^*/a = radius ratio at the change in constant occurs = 1.89

a^* = radius at which the adiabatic constant changes

It is advantageous to normalize equations (3.12), (3.13) and (3.16) by the modulus E. The normalized equations are developed below. Equation (3.12) becomes:

$$\left(\frac{Y}{E\alpha}-\frac{q}{E}\right)\left(\frac{b}{a}\right)^{\alpha/(1+\alpha)}-\frac{Y}{E\alpha}-\frac{p(a)}{E}=0 \qquad (3.17)$$

Equation (3.13) becomes:

$$\frac{q}{E}=-\frac{\frac{Y_2}{E}+2\frac{P}{E}(1+\alpha_2)}{2+\alpha_2} \qquad (3.18)$$

Equations (3.16a) and (3.16b) become:

$$\frac{p(a)}{E}=\frac{P_o}{E}\left(\frac{a}{a_o}\right)^{-2\gamma_1}, \quad a\le a^* \qquad (3.19a)$$

and

$$\frac{p(a)}{E}=\frac{P_o}{E}\left(\frac{a^*}{a_o}\right)^{-2\gamma_1}\left(\frac{a}{a^*}\right)^{-2\gamma_2}, \quad a\ge a^* \qquad (3.19b)$$

The remaining equations are normalized with respect to a_o. Equation (3.14) becomes:

$$\frac{u_b}{a_o} = -(1+\nu)\frac{b}{a_o}\frac{[q+2P(1-\nu)])}{E} \qquad (3.20)$$

and Equation (3.15) becomes:

$$\left(\frac{a}{a_o}\right)^2 - 1 = \left(\frac{b}{a_o}\right)^2 - \left[\frac{b}{a_o} - \frac{u_b}{a_o}\right]^2 \qquad (3.21)$$

The following calculation procedure is used:

- *q/E* is calculated from equation (3.18).
- A value of b/a_o is estimated.
- The b/a_o value together with q/E is substituted into equation (3.20), then u_b/a_o is calculated.
- The result is substituted into equation (3.21) and a/a_o is calculated.
- The value of a/a_o is compared with a^*/a_o = 1.89. Based upon the comparison, the appropriate pressure equation (3.19a) or (3.19b) is chosen to obtain *p(a)/E*.
- Th *p(a)/E* value is then substituted into equation (3.17). If the equality is satisfied within acceptable limits (1 pct), the design is done. If not, the second step is returned to and another b/a_o is selected.

The Sher procedure is easily handled using a spreadsheet.

To be consistent with the other approaches, it is desirable to present a simple set of design curves. As can be seen, there are a number of different input parameters involved and thus some decisions have been taken to obtain a more or less representative set of values from literature [15] and experience. The following were selected:

$$\frac{\sigma_c}{c} = 5$$

$$\frac{E}{\sigma_c} = 300$$

$$\frac{\sigma_c}{\sigma_t} = 12$$

The remaining parameter are

$\varphi = 42^o$

$\upsilon = 0.3$

$a_o = r_h = 0.0225$m

$\rho_r = 2650$ kg/m^3

P = in situ stress = 0

The in situ stress P is set to zero for simplicity. If the in situ stress were applied, the result would be a reduction in the calculated damage limit. Hence, by using P=0, a more conservative estimate results.

The ratio:

$$\frac{R_d}{r_h} = \frac{b}{a_o}$$

was determined for different combinations of the rock compressive strength (σ_c) and the explosive pressure (P_o). Figure 9 presents the results.

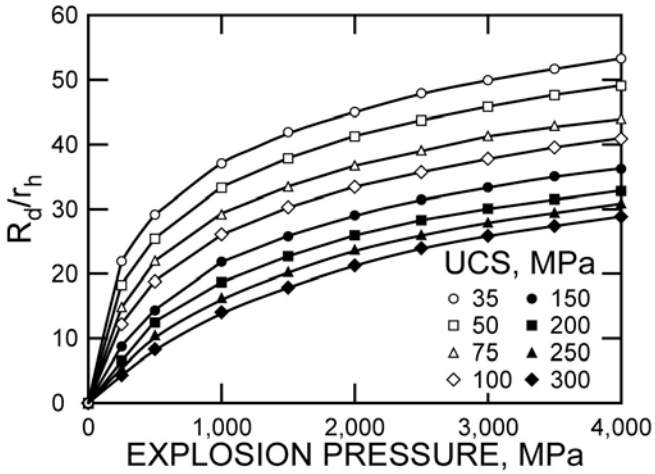

Figure 9. The design charts when using the Sher approach.

It can be seen the results are generally consistent with those produced using the other approaches. An advantage with the Sher approach is that different rock parameters can be specifically included. The requirement for rock parameters is also a disadvantage if they are not available.

4. EVALUATION OF A SUCCESSFUL CONTROLLED BLAST DESIGN

Figure 10 shows a successful controlled blast design currently being applied at a mine. It will serve as the basis for analysis using the buffer row concept, since the position of the buffer row is parallel to the perimeter and approximately at the correct damage distance from the perimeter. It is considered a successful design because the as-designed is equivalent to the as-drilled and as-built. Damage beyond the as-built limit is subjective since no measure of radial cracks was made. Overbreak has been minimized and the perimeter is defined by the perimeter blast hole half barrels.

The basis used for the design, especially the buffer row distance from the perimeter, is uncertain. It may in fact be based on a standard empirical-based design or a special design from the mine's expert consultant. The

provided successful design was selected to illustrate one that best follows the buffer row design.

The site was visited by the author and the required geotechnical and design data were supplied by the mine. The round was drilled using a computer-controlled drill jumbo. The round was charged using site sensitized emulsion (SSE). The charging rig had string loading capability in charging the perimeter holes. The following is a comprehensive list of parameters that were available for the example:

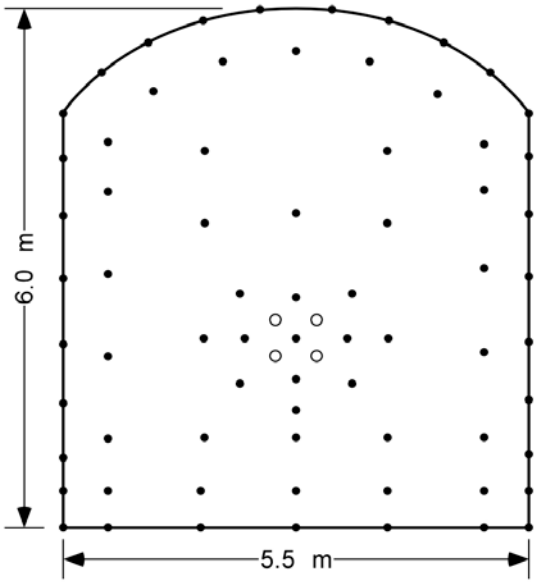

Figure 10. The blast design used as an example showing the drilled design at the face.

Explosive Properties

- Type: SSE
- Energy: 3.1 MJ/kg = 740 kcal/kg
- Gas volume: about 950 l/kg
- Density: 0.85 g/cm^3
- *VOD*: 4,300 m/s
- Relative weight strength (*RWS*): s_{ANFO} = 0.84
- Buffer holes: fully charged
- Perimeter holes: string loaded to 50% of hole cross-sectional area
- Adiabatic constant assumed: γ = 3.0

Geometry

- Hole diameter: 48 mm
- Hole length: 6 m
- Drift width: 5.5 m
- Drift height (shoulder): 4.8 m
- Drift height (crown): 6 m
- Drift cross-sectional area: 31 m^2
- Buffer row spacing: 0.94 m
- Buffer row burden: 1.1 m
- Perimeter row spacing: 0.66 m
- Perimeter row burden: 0.56 m

Rock Properties

- Volcanic rock type: monzonite
- Density: 2.8 g/cm^3
- Young's modulus: 72,000 MPa
- Poisson's ratio: 0.28
- P-wave velocity: 5,900 m/s
- Unconfined compressive strength: 150 MPa
- Tensile strength: 22 MPa (Brazilian test)
- Friction angle = 45°

4.1. *Application of the Modified Ash Energy-based blast damage model*

The basic equation (3.5) is:

$$\frac{R_d}{r_h} = 25\sqrt{\frac{\rho_e s_{ANFO}}{\rho_{ANFO}}}\sqrt{\frac{2.65}{\rho_{rock}}} = 25\sqrt{\frac{0.85(0.84)}{0.85}}\sqrt{\frac{2.65}{2.8}} =$$
$$= 25(0.92)(0.97) = 22.3$$

The buffer hole damage radius then becomes:

$$R_d = 22.3(0.024) = 0.54\ m$$

For the perimeter holes, equation (3.9) includes the effect of de-coupled charges:

$$\frac{R_d}{r_h} = 25\left(\frac{d_e}{d_h}\right)\sqrt{\frac{\rho_e s_{ANFO}}{\rho_{ANFO}}}\sqrt{\frac{2.65}{\rho_{rock}}}$$

As indicated, string loading is used in the perimeter holes with about 50% of the cross-sectional area filled with explosive. The equivalent explosive diameter d_e is determined using:

$$\frac{\pi}{4}d_e^{\,2} = (0.50)\frac{\pi}{4}d_h^{\,2}$$

$$d_e = d_h\sqrt{0.5} = 0.707 d_h = 0.707(0.048) = 0.034m$$

Thus, the coupling (*Cpl*) is:

$$Cpl = \frac{d_e}{d_h} = \frac{0.034}{0.048} = 0.71$$

Substituting the appropriate values, one obtains:

$$\frac{R_d}{r_h} = 25(0.71)\sqrt{\frac{0.85(0.84)}{(0.85)}}\sqrt{\frac{2.65}{2.80}} =$$
$$= 25(0.71)(0.92)(0.97) = 15.8$$

The expected perimeter hole damage radius is:

$$R_d = 15.8(0.024) = 0.39\ m$$

4.2. *Application of the Modified Ash Pressure-based blast damage model*

Rock properties for the modified Ash pressure-based damage model are simply the rock density. The approach is discussed in Hustrulid [16] and supported by the work of Ash [5, 6, 7, 8]. The basic equation (3.11) for calculating the damage radius for fully coupled holes using the Modified Ash pressure-based approach is:

$$\frac{R_d}{r_h} = 25\sqrt{\frac{P_e}{P_{ANFO}}}\sqrt{\frac{2.65}{\rho_{rock}}}$$

where

R_d = damage radius, m

r_h = hole radius, m

P_e= explosion pressure, MPa

ρ_{rock} = rock density, g/cm^3

P_{ANFO} = explosion pressure for ANFO, MPa

It will be assumed that the explosion pressure P_e is calculated using:

$$P_e = \frac{1}{8}\rho_e (VOD)^2 \qquad (4.1)$$

where:

ρ_e = 850 kg/m^3

Velocity of Detonation (VOD)= 4.3 km/s

Thus,

$$P_e = \frac{1}{8}\rho_e (VOD)^2 = \frac{1}{8}(850)(4.3)^2 = 1965\ MPa$$

Using P_{ANFO} = 1,300 MPa and ρ_r = 2.8 g/cm^3, one finds that:

$$\frac{R_d}{r_h} = 25\sqrt{\frac{P_e}{P_{ANFO}}}\sqrt{\frac{2.65}{\rho_{rock}}} = 25\sqrt{\frac{1965}{1300}}\sqrt{\frac{2.65}{2.8}} = 29.9$$

The buffer hole damage radius then becomes:

$$R_d = 29.9(0.024) = 0.72\ m$$

The appropriate equation for calculating the damage radius for the perimeter holes is:

$$\frac{R_d}{r_h} = 25\sqrt{\frac{P_{e\ wall}}{P_{ANFO\ wall}}}\sqrt{\frac{2.65}{\rho_{rock}}} \qquad (4.2)$$

It is necessary to determine the wall pressure for the de-coupled charge. The co-volume approach will be demonstrated here. The specific volume (υ_e) for the explosive is:

$$\nu_e = \frac{1}{\rho_e} = \frac{1}{0.85} = 1.176$$

The volume term (V_e) considering the co-volume correction is:

$$V_e = \nu_e - 1.1\,e^{\frac{-0.473}{\nu_e}} = 1.176 - 1.1\,e^{\frac{-0.473}{1.176}} =$$
$$= 1.176 - 0.736 = 0.440$$

The specific volume for the explosive gases in the hole is:

$$\nu_h = \nu_e\left(\frac{d_h}{d_e}\right)^2 = 1.176\left(\frac{0.048}{0.034}\right)^2 = 2.344$$

The volume term (V_h) considering the co-volume correction is:

$$V_h = \nu_h - 1.1\,e^{\frac{-0.473}{\nu_h}} = 2.344 - 1.1\,e^{\frac{-0.473}{2.344}} =$$
$$= 2.344 - 0.899 = 1.445$$

The wall pressure ($P_{e\ wall}$) then becomes:

$$P_{e\ wall} = P_e\left(\frac{V_e}{V_h}\right) = 1965\left(\frac{0.440}{1.445}\right) = 598\ MPa$$

Thus,

$$\frac{R_d}{r_h} = 25\sqrt{\frac{P_{e\ wall}}{P_{ANFO\ wall}}}\sqrt{\frac{2.65}{\rho_{rock}}} = 25\sqrt{\frac{598}{1300}}\sqrt{\frac{2.65}{2.80}} =$$
$$= 25(0.68)(0.97) = 16.5$$

The expected perimeter hole damage radius is:

$$R_d = 16.5(0.024) = 0.40\ m$$

4.3. *Application of the Sher quasi-static blast damage model*

As indicated, Sher is the most complicated of the approaches presented and a spreadsheet is used for making the calculations. The cohesion (c) of the rock has not been given and it will be assumed that it is:

$$c = \frac{\sigma_c}{5} = \frac{150}{5} = 30\ MPa$$

It is also assumed that the effect of the in situ stress (P) can be neglected. The zero pressure assumption is needed for comparison of results from the Ash models. Applying the in situ stress in the Sher model will reduce the damage radius. Indicated below are the values for the different ratios and parameters used in the solution:

$$\alpha = \frac{2\sin\phi}{1-\sin\phi} = \frac{2\sin(45^o)}{1-\sin(45^o)} = 4.828$$

$$Y = \frac{2c\cos\phi}{1-\sin\phi} = \frac{2(30)\cos(45^o)}{1-\sin(45^o)} = 145MPa$$

$$\alpha_2 = \frac{\sigma_c}{\sigma_t} - 1 = \frac{150}{22} - 1 = 6$$

$$Y_2 = \sigma_c = 150MPa$$

$$\frac{Y_2}{E} = \frac{150}{72000} = 0.00208$$

$$\frac{P}{E} = 0.0$$

$$\frac{Y}{E} = \frac{145}{72000} = 0.00201$$

$$\frac{P_o}{E} = \frac{1965}{72000} = 0.0273$$

These values are substituted into the appropriate equations using an estimated b/a_o (the damage radius/hole radius). The ratio of b/a_o that satisfies the system of equations is selected. In this particular case, it is found that:

$$\frac{R_d}{r_h} = \frac{b}{a_o} = 28$$

The buffer hole damage radius then becomes:

$$R_d = 28(0.024) = 0.67\ m$$

The Sher approach is not easily applied for de-coupled charges since it requires knowing the adiabatic expansion constant for the reduced pressure applied to the borehole wall. Here, the limiting condition will be used. Assuming that:

$$\gamma = 3$$

and introducing the wall pressure:

$$P_{e\ wall} = 598 \text{ MPa}$$

one finds that:

$$\frac{R_d}{r_h} = 18$$

The expected damage radius is:

$$R_d = 18(0.024) = 0.43\ m$$

4.4. *Comparison of blast damage calculations*

Table 1 presents the results for the buffer holes and the perimeter holes using the different techniques. As might be expected, the different approaches yield somewhat different estimates of the damage radius.

Table 1.Summary of the buffer and perimeter hole results

Practical damage radius approach	*Buffer*		*Perimeter*	
	R_d/r_h	R_d,m	R_d/r_h	R_d ,m
Modified Ash energy-based	22.3	0.54	15.8	0.39
Modified Ash pressure-based	29.9	0.72	16.5	0.40
Sher quasi-static	28	0.67	18	0.43

There is good agreement in the perimeter hole results with an average R_d = 0.41 m. There is less agreement in the buffer hole R_d with a range from 0.54 m to 0.72 m and averaging 0.64 m.

The average R_d practical damage circles have been drawn around the buffer and perimeter holes as shown in Figure 11.

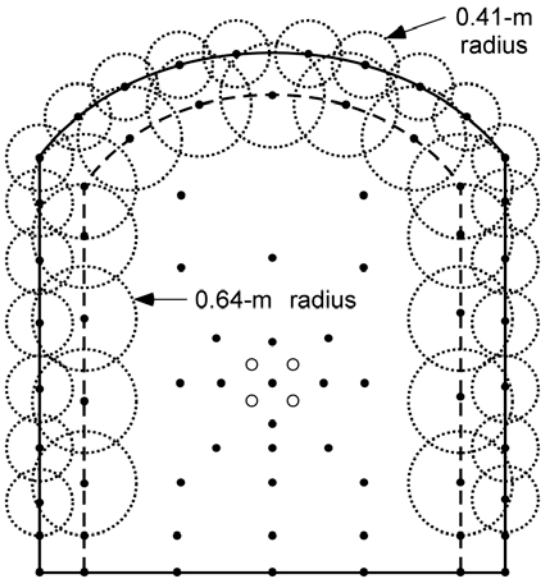

Figure 11. Overlay of the damage radius circles R_d around the buffer and perimeter holes.

The successful design here might imply that there is no improvement needed. However, analysis of the design does show several important relationships using the applied average R_d practical damage radius including:

- The designed perimeter burden (buffer hole R_d) = 0.54 m.
- The calculated average buffer hole R_d of 0.64 is greater than the designed perimeter burden.

- The perimeter holes look out and look up resulting in a larger opening at the end of the blast round, indicating a successful range in the R_d value.
- The designed perimeter burden (buffer hole R_d) at the end of the blast round is about 1.0 m.
- The buffer hole spacing is 0.85 m or 1.57 times the designed R_d = 0.54 m, and is slightly larger than the suggested buffer hole spacing of $1.3R_d$ to $1.5R_d$.
- The perimeter hole spacing is 0.65 m and is less than the suggested buffer design concept of $1.3R_d$ to $1.5R_d$ or 0.83 m to 0.96 m, based on the calculated average buffer hole R_d alternating with the buffer hole spacing.
- The successful perimeter spacing results in "just touching practical damage circles" indicating possibly that circle coverage is a requirement for clearing/smoothing the perimeter.
- Twenty-two perimeter holes and 15 buffer holes, or a ratio of 1.47:1 perimeter to buffer, was successful

The results of the analysis would suggest some modifications in the buffer row concept, including:

- A determination if the buffer hole R_d should be assigned to the maximum, the minimum, or the average perimeter burden (buffer hole R_d).
- The buffer hole R_d spacing concept of $1.3R_d$ to $1.5R_d$ may be too small where a larger ratio of 1.57 was satisfactory.
- Spacing of the perimeter holes at the cusps, which is part of the buffer row design concept, may not be adequate. Locating the perimeter holes between the existing buffer holes would result in a larger spacing than used in the successful design. A total of 16 holes at the cusps and two at the abutment corners would be required for the conceptual design using existing buffer hole locations. The addition of perimeter holes at the buffer hole R_d tangent would effectively double the concept requirements for perimeter holes. Instead of 24 perimeter holes as in the successful design, the modified buffer hole concept would require 16 holes at the cusps and 15 holes at the tangent for a total of 31 perimeter holes.
- Alternatively, the successful perimeter spacing could drive the buffer spacing. A reduced buffer hole spacing from the successful design should be as effective. Thus, the perimeter spacing of 0.65 m is equivalent to $1.2R_d$ where R_d = 0.54 and the suggested buffer spacing is redefined.
- The "just touching practical damage circles" of the perimeter holes in the successful design suggests correct spacing, yet, as described earlier (Figure 5), the practical damage radius is less than the radial crack extent. The radial cracks between perimeter holes should extend beyond the practical damage radius and intersect/connect suggesting a lesser charge or a more increased spacing than designed.

In summary, the average calculated buffer row R_d of 0.64 proved to be within the range of the successful perimeter burden ranging from 0.54 m to 1.0 m. Conversely, there was only a reasonable comparison between the number and location of the perimeter holes in the successful design compared to the number of perimeter holes and cusp locations required using the buffer row design concept. Possibly the perimeter holes could be placed more for drilling convenience rather than being located at the cusps.

5. EVALUATION OF A SECOND SUCCESSFUL BLAST DESIGN

The mine geology consists of quartz vein stock works. The rock mass quality was determined to have an RMR of 48. The drift design (Figure 12) is nominally 4.27 m by 4.27 m in cross-section with an arched roof, and the abutment height is 2.135 m. A line of buffer holes parallels the perimeter holes defining a perimeter burden of 0.76 m . Blast holes are 1-7/8 inch (0.048-m) diameter. The production holes are charged with ANFO and are drilled on a 34-in (0.86-m) by 36-in (0.9-m) grid. A detonator and booster are used for initiation. For perimeter control, ANFO is used for the back perimeter holes by charging the bottom third of the hole and leaving the upper two-thirds of the hole empty. The result is a decrease in the overall charge over the entire length of the hole, yet the bottom third is fully coupled. A calculation was made to determine the practical damage distance for the uncharged length based on the explosive gas expanded into that section.

The buffer row is shown as a painted line inset from the painted perimeter in Figure 13.

5.1. *Buffer*

Using the modified Ash pressure-based approach, the ANFO blast hole wall pressure (1300 MPa) and the rock density (2.60 g/cm^3) are used to calculate the expected damage radius ratio, as follows:

$$R_d / r_h = 25\sqrt{\frac{P_{eExp}}{P_{eANFO}}}\sqrt{\frac{\rho_{rock}}{2.65}} = 25\sqrt{\frac{1300}{1300}}\sqrt{\frac{2.65}{2.60}} = 25.2$$

Since the blast hole radius is r_h = 0.9375 in (0.0238 m), the value of R_d for the ANFO fully coupled buffer holes becomes:

$$R_d = 0.60 \text{ m}$$

5.2. *Perimeter*

The reduced pressure in the empty portion of the perimeter hole was determined to be 249 MPa. The damage radius ratio for the back perimeter holes is given by equation (3.11):

$$\frac{R_d}{r_h} = 25\sqrt{\frac{P_{e\ wall}}{1300}}\sqrt{\frac{2.65}{\rho_{rock}}} = 25\sqrt{\frac{249}{1300}}\sqrt{\frac{2.65}{2.60}} = 11.0$$

The value of R_d for the right rib perimeter using ANFO bottom-charged becomes:

$$R_d = 0.26 \text{ m}$$

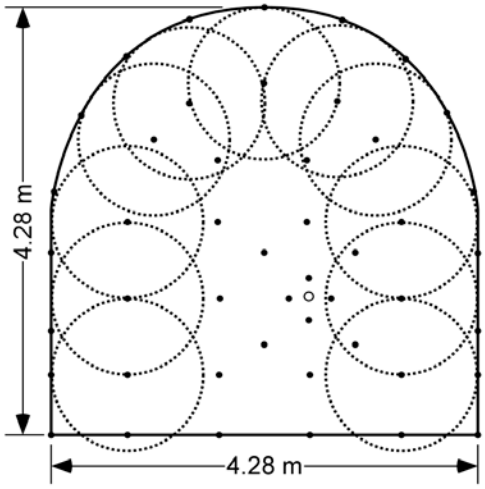

Figure 12. Second mine blast design showing buffer hole damage circles extending across the 0.76-m perimeter burden.

Figure 13. The buffer row design painted on the face.

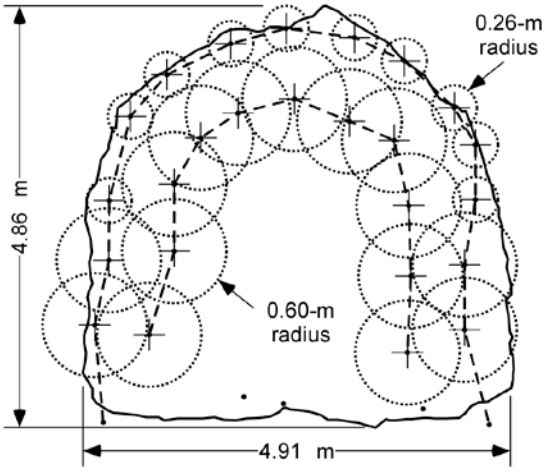

Figure 14. Vertical section at mid-round showing final perimeter and calculated buffer row and perimeter damage circles. The rib perimeter holes were fully coupled.

5.3. *Results*

The mine design employs a common control practice of bottom charging the perimeter holes to reduce the explosion energy and in turn reducing perimeter damage. Though not as effective as a full-length decoupled charge, bottom charging does reduce damage compared to fully coupled charging and can be considered a successful blast design.

We can assess the important relationships between the calculated R_d practical damage radius and the measured overbreak damage based on these observations:

- The overbreak measure for the back ranged from 0.04 m to 0.26 m and averaged 0.10 m.
- The left rib overbreak ranged from 0.05 m to 0.18 m performing in a similar way to the bottom-charged back holes.
- The right rib overbreak ranged from 0.17 to 0.59 m. The excessive right rib overbreak was as expected from fully coupled charges. In addition, there were near-vertical joint structures paralleling the heading along the right rib contributing to the damage.
- The as-designed buffer row damage radius of 0.76 m was not met at the ribs. The calculated damage circles (0.60 m) were nearly tangent to the as-drilled perimeter holes in these cases.
- Perimeter hole R_d circles are generally "not touching" yet provide adequate smoothing of the perimeter. The average as-drilled perimeter hole spacing along the back was 0.78 m.

The successful design yields the following results:

- The average as-drilled buffer hole spacing at mid-round was 0.66 m. The spacing becomes $0.86R_d$ where R_d is the designed 0.76 m.

- Ten perimeter holes and seven buffer holes for the back section, or a ratio of 1.4:1 perimeter: buffer ratio, was successful. The average spacing was 0.78 m.
- The mines R_d is greater than that of the buffer hole design concept R_d using the modified Ash pressure-based approach.

The successful design required closer spacing of the buffer holes and a larger $R_{d,}$ practical damage distance. The number of perimeter holes in the mine's design was greater than what would be expected for the buffer design concept if the buffer hole spacing were deemed correct.

The buffer hole spacing could be extended, similar to the successful rib buffer hole spacing (0.86 m), to meet the buffer hole concept requirement using the successful perimeter spacing in the back (0.78 m).

In summary, the successful design provides additional insight into possible adjustments for the buffer row design concept. A buffer hole spacing less than the conceptual range of $1.3R_d$ to $1.5R_d$ might be tried. The successful perimeter hole spacing would then align with the new buffer hole cusp locations.

6. CONCLUSIONS

Poor blasting practices can result in excessive overbreak and rock damage and are a possible contributing factor in many fall-of-ground accidents. Today, available drilling and blasting technology has developed to the point that there is no reason why the rock mass cannot be "cut as with a knife" if so desired (Kvapil, 2008). One of the missing items in the overall process is a simple, but technically sound, method for assigning the damage radius produced by a particular explosive-hole-rock combination. The authors suggest that the proper design of the buffer row of blast holes is the key to successful perimeter control. Perimeter control translates into improved safety and better economy, both of which are essential to modern mining.

Controlled blasting is not a new concept. Nevertheless, by using the buffer row design concept, mines can understand how damage affects the perimeter and how to use that knowledge in the design process. The authors suggest that mines evaluate their drifting blast designs based on perimeter control. Questions to consider include:

- Are fully coupled charges used for perimeter holes defining the final designed perimeter?
- Is the as-built drift geometry including height and width greater than the design and as-drilled expectations?
- Could the mine save time and reduce exposure of miners during scaling by improving perimeter control?
- Is there additional muck being handled due to overbreak that could be reduced by improving perimeter control?

Answering yes to any or all of these questions indicates a need to apply better blasting strategies. The buffer row concept is one option for achieving better perimeter control.

The buffer design concept applying the calculated R_d was analyzed using two successful blast designs. The findings are that:

- the successful designs have a buffer row that parallels the perimeter;
- the successful designs have closer perimeter spacing than indicated in the initial buffer design concept;
- the buffer row hole spacing used in the two successful designs compare reasonably with the suggested spacing using the buffer row design concept.

The following is a simple process for developing the experience needed to determine the optimum practical damage limit for design:

- Evaluate current blast design practices for overbreak problems.
- Ask the question: Is there a need to improve perimeter control?
- Calculate a practical damage limit for production holes using one of the three methods provided.
- Design a blast round using the buffer hole algorithm principle.
- Conduct trial blasts.
- Observe results.
- Adjust the practical damage radius.
- Conduct additional trial blasts.

7. REFERENCES

1. Iverson, S., W. Hustrulid, J. Johnson, M. Kuchta. 2010. Drift Software 1.0 (BETA) and User Manual (DRAFT), NIOSH Internal Report, Available from Authors, Spokane, WA, 112 pp

2. Holmberg, R. 1982. Charge Calculations for Tunneling., Underground Mining Methods Handbook, Hustrulid, W., editor, AIME, New York, pp. 1580-1589.

3. Hustrulid, W. and J. Johnson. 2008. A Gas Pressure-based Drift Round Blast Design Methodology, Proceedings, Mass Min 2008, 5th International Conference & Exhibition on Mass Mining, Luleå, Sweden, pp. 657-669.

4. Tesarik, D.R., and W.A. Hustrulid, and U. Nyberg. 2011. Assessment and application of a single charge-blast test at the Kiruna mine, Sweden, NIOSH internal report, Spokane, Wa.

5. Ash, R.L. 1963. The mechanics of rock breakage Part 1. Pit and Quarry, 56(2):98-100.

6. Ash, R.L. 1963. The mechanics of rock breakage Part 2 – Standards for blasting design. Pit and Quarry, 56(3):118-122.

7. Ash, R.L. 1963. The mechanics of rock breakage Part 3 – The characteristics of explosives. Pit and Quarry, 56(4):126 - 131.

8. Ash, R.L. 1963. The mechanics of rock breakage Part 4 – Material properties, powder factor, blasting cost. Pit and Quarry, 56(5):109-118.

9. Hustrulid, W. 1999. Blasting Principles for Open Pit Mining, Volume 1 – General Design Concepts, A.A.Balkema/Rotterdam/Brookfield, 382 pp.

10. Hustrulid, W. 1999. Blasting Principles for Open Pit Mining, Volume 2 – Theoretical Foundations, A.A.Balkema/Rotterdam/Brookfield, 1013 pp.

11. Hustrulid, W.A. 2007. A Practical, Yet Technically Sound, Design Procedure for Pre-Split Blasts, Proceedings of the Thirty-Third Annual Conference on Explosives and Blasting Technique, International Society of Explosives Engineers, Nashville, TN USA, 26 pp.

12. Sher, E.N. 1997. Taking into Account the Dynamics in Description of Fracture of Brittle Media by an Explosion of a Cord Charge, Journal of Applied Mechanics and Technical Physics, Vol. 38, No. 3, pp. 484-492.

13. Sher, E.N., and N.I. Aleksandrova. 1997. Dynamics of development of crushing zone in elasto plastic medium in camouflet explosion of string charge, Journal of Mining Science, Vol. 33, No. 6, pp. 529-535.

14. Sher, E.N., N.I. Aleksandrova, M. Ayzenberg-Stepanenko, and A.G. Chernikov. (2007) Influence of the block-hierarchical structure of rocks on the peculiarities of seismic wave propagation. Journal of Mining Science, Vol. 43, No. 6, pp. 585 - 591.

15. Deere, D.U. 1968. Geological Considerations in Rock Mechanics in Engineering Practice, Stagg, K. G., and O. C. Zienkiewicz, (ed.), John Wiley & Sons, pp. 1-20.

16. Hustrulid, W. 2010. Some Comments Regarding Development Drifting Practices with Special Emphasis on Caving. Proceedings, Caving 2010. The Second International Symposium on Block and Sublevel Caving, Yves Potvin, editor, Australian Centre for Geomechanics, pp 3-44.

17. Kvapil, R. 2008. Personal Communication.